

AIE (AIEE) and mechanofluorochromic performances of TPE-methoxylates: effects of single molecular conformation†

Cite this: *RSC Advances*, 2013, 3, 7996

Qingkai Qi,^a Yifei Liu,^{*b} Xiaofeng Fang,^b Yumo Zhang,^a Peng Chen,^a Yi Wang,^a Bing Yang,^a Bin Xu,^a Wenjing Tian^a and Sean Xiao-An Zhang^{*a}

Two methoxy-substituted tetraphenylethylene (TPE) derivatives, tetra(4-methoxyphenyl)ethylene (TMOE) and tetra(3,4-dimethoxyphenyl)ethylene (TDMOE), were synthesized by McMurry reaction in high yields. The nearly centrosymmetric and natural propeller shape of TMOE and TDMOE excluded intermolecular effects, such as H or J-aggregation and π - π stacking, on their AIE (AIEE) and mechanofluorochromic performance. The crystal structures of TMOE and TDMOE, and theoretical calculations proved that their emission colours are determined by single molecular conjugation. These molecules were used to investigate pure conformational effects on molecular emissions. The spectral properties of these molecules in five environments of crystal(s), THF solution, THF–water binary solution, solidified THF and amorphous states, were investigated. The crystalline to amorphous phase transition by grinding resulted in good mechanofluorochromic performances with high quantum yields and distinguishable emission change, which was further explored as anti-counterfeiting inks on banknotes.

Received 11th February 2013,
Accepted 15th March 2013

DOI: 10.1039/c3ra40734a

www.rsc.org/advances

1. Introduction

Tetraphenylethylene (TPE) derivatives are hotly investigated in recent years for their aggregation induced emission (AIE) or aggregation induced emission enhancement (AIEE) properties.¹ AIE or AIEE refer to the organic molecules which are practically non-luminescent or weakly luminescent in solution but become strongly emissive in aggregated states, because the non-irradiation transitions from the free rotation of the single bonds in the conjugation system are forbidden.² AIE (AIEE) materials are very important in developing efficient organic light emitting devices (OLED) and bio-labels.³ Recent studies show that some TPE derivatives possess solid state mechanofluorochromic performances, which means the materials have different fluorescent emissions upon mechanical force.⁴ As a kind of “smart material”, mechanofluorochromic

materials have vast applications in pressure sensors, rewritable media and security ink.⁵ In previous work, large aromatic groups were usually introduced on TPE motif to enable the tunable mechanofluorochromic properties. It has been revealed that the mechanofluorochromic performances of TPE derivatives are related to the crystalline to amorphous phase transition.⁶ However, the inherent reasons for emission shift is hard to elucidate in amorphous state. Changes in intramolecular planarity,^{4a,7} as well as intermolecular interactions of π - π stacking,⁸ and H or J-aggregation⁹ have all been assigned as the causes of mechanofluorochromic phenomena. Whereas, the mechanism is very critical in molecular design, which determines the mechanofluorochromic performances of the materials, such as color contrast and quantum efficiency. Another question is what structures can have crystalline to amorphous phase transition and the resultant mechanofluorochromic properties, because it is found that not all TPE derivatives have the phase transition.⁶ Resolving these questions needs more studies on a wider library of objects, more reasonable designs and characterizations.

Most recently, Dong and Tang *et al.* reported much simpler ethoxy- and butoxy-substituted TPE, and demonstrated their morphology-dependent multi-color emissions by different external stimuli in solid state.¹⁰ Due to the natural propeller shape, intermolecular stacking, such as π - π stacking and H or J-aggregation, is unlikely to happen in these molecules, which offered simpler models for AIE (or AIEE) and mechanofluorochromism study. In this article, two even smaller methoxy-

^aState Key Lab of Supramolecular Structure and Materials, College of Chemistry, Jilin University, Changchun, 130012, P. R. China. E-mail: seanzhang@jlu.edu.cn; Fax: +86-0431-85153812

^bCollege of Chemistry, Jilin University, Changchun, 130012, P. R. China. E-mail: liuyifei@jlu.edu.cn; Fax: +86-0431-85153812

† Electronic supplementary information (ESI) available: Characterizations and single crystals of TMOE, TDMOE and TPE. Torsion angle data, theoretical calculation data, and DSC of TMOE-1 and TMOE-2. Mechanofluorochromic cycles of TMOE treated by grinding and solvent treatment. PL spectra and powder X-ray diffraction patterns of TPE crystal before and after grinding. Analysis of the weak interactions in single crystal structures of TMOE-1, TMOE-2, TDMOE and TPE. CCDC reference numbers 921515, 921516. For ESI and crystallographic data in CIF or other electronic format see DOI: 10.1039/c3ra40734a

substituted TPE derivatives were synthesized, which are tetra(4-methoxyphenyl)ethylene (TMOE) and tetra(3,4-dimethoxyphenyl)ethylene (TDMOE). Two different crystal structures of TMOE with different emission colours were obtained, which prove that their emissions are determined by single molecular conformation (or conjugation state). Therefore, these molecules provide ideal objects to investigate pure conformational effects on molecular emissions. Crystal(s), THF solution, THF–water binary solution, solidified THF and amorphous states were used as five environments to induce conformational change and emission response. The crystalline to amorphous phase transition of TMOE and TDMOE by grinding resulted in good mechanofluorochromic performance. In the absence of intermolecular effects, they both have high quantum yields (TMOE >50%, TDMOE >70%) before and after grinding. Well distinguishable colour contrast with emission peak shift of 60 nm and 20 nm were obtained for TMOE and TDMOE, respectively. Moreover, utilizing its mechanofluorochromic property, TMOE was demonstrated as an anti-counterfeiting ink for banknotes.

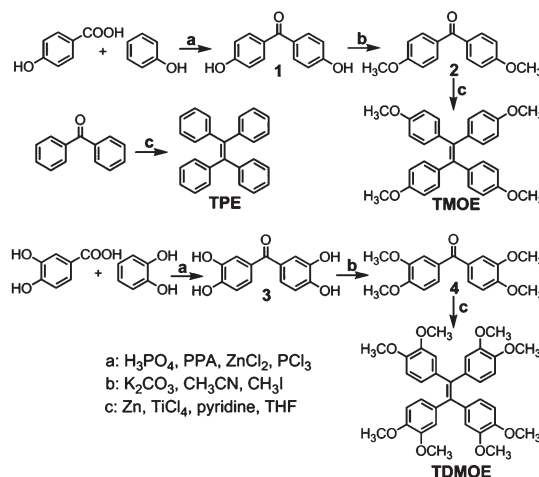
2. Experimental section

2.1 Materials

Acetonitrile was purchased from Xilong Chemical Reagent. K_2CO_3 , phenol and H_3PO_4 were purchased from Beijing Chemical Plant. $ZnCl_2$, polyphosphoric acid (PPA, $P_2O_5 \geq 80\%$) and iodomethane were purchased from Sinopharm Chemical Reagent. PCl_3 was purchased from Tianjin Guangfu Chemical Reagent. 3,4-Dihydroxy benzoic acid, *p*-hydroxy benzoic acid, 1,2-benzenediol, benzophenone, Zn dust, $TiCl_4$ and dry pyridine were all purchased from Aladdin. All the above chemicals were of analytical grade and used as received without further purification. Tetrahydrofuran (THF) was distilled in presence of sodium benzophenone under protection of dry nitrogen prior to use.

2.2 Synthesis

The synthetic routes of TMOE, TDMOE and TPE are illustrated in Scheme 1. The diaryl methanones (**1**, **2**, **3**, **4**) were prepared according to the literature (see ESI†). TMOE was synthesized by McMurry reaction:¹¹ $TiCl_4$ (0.6 mL, 5.4 mmol) was added dropwise to chilly ($\sim 0^\circ C$) anhydrous tetrahydrofuran (20 mL) under nitrogen atmosphere. Then Zn dust (0.702 g, 10.8 mmol) and dry pyridine (20 μ L, 0.25 mmol) were added to the mixture immediately. The black suspension was warmed to room temperature and then refluxed for 2 h. A solution of **2** (2 mmol) in 5 mL THF was added slowly into the above mixture during refluxing. The reaction was finished until **2** were completely consumed (monitored by TLC). The mixture was cooled to room temperature and quenched with aqueous K_2CO_3 (5 mL, 10%). The organic layer was separated and the aqueous suspension was extracted with dichloromethane (4×25 mL). The organic phase was dried with anhydrous $MgSO_4$. The crude products were purified by recrystallization (methanol/dichloromethane) to get crystals with a yield about 85%. TDMOE and TPE were synthesized with similar protocols and



Scheme 1 Synthetic routes for TMOE, TDMOE and TPE.

the yields were about 74% and 86%. Detailed characterizations of the three compounds are listed in the ESI.† Crystals of TPE and TDMOE were both grown from their methanol/dichloromethane solutions. Two different crystals of TMOE (denoted as TMOE-1 and TMOE-2) were grown from its n-hexane/dichloromethane and methanol/dichloromethane solution, respectively.

2.3 Instruments

1H NMR spectra were recorded on a 500 MHz Bruker Avance or a Varian-300 EX spectrometer using $CDCl_3$ or $DMSO-d_6$ as solvent and tetramethylsilane (TMS) as an internal standard ($\delta = 0.00$ ppm). ^{13}C NMR spectra were recorded on a Bruker Avance 500 MHz spectrometer using $CDCl_3$ as solvent and $CDCl_3$ as an internal standard ($\delta = 77.00$ ppm). UV-Vis spectra were measured on a Shimadzu UV-2550 spectrophotometer. Photoluminescence (PL) spectra were measured with a RF-5301PC spectrofluorometer. Powder XRD patterns were obtained from a PANalytical B.V. Empyrean X-ray diffractometer with $Cu-K\alpha$ radiation ($\lambda = 1.5418 \text{ \AA}$) at $25^\circ C$ (scan range: $4\text{--}50^\circ$). Single crystal X-Ray analyses were performed on a RAXIS RAPID-F X-ray single crystal diffractometer. DSC experiments were recorded on a NETZSCH DSC 204 instrument at a scanning rate of 10 K min^{-1} . The fluorescence lifetime measurements were performed on a time-correlated single-photon counting (TCSPC) system under right-angle sample geometry using mini- τ miniature fluorescence lifetime spectrometer (Edinburgh Instruments). A 379 nm picosecond diode laser (Edinburgh Instruments EPL-375, repetition rate 5 MHz, 64.8ps) was used to excite the samples. Crystalline and amorphous state PL quantum yields were measured with an integrating sphere (C-701, Labsphere Inc.) with a 405 nm Ocean Optics LLS-LED as the excitation source, and the light was introduced into the integrating sphere through an optical fiber.

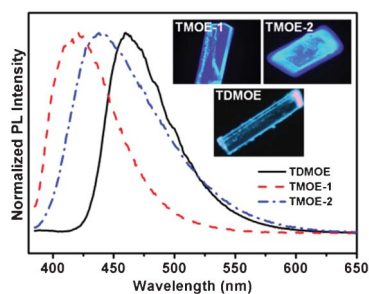


Fig. 1 Normalized PL spectra of TMOE-1, TMOE-2 and TDMOE crystals. Inset: microscopic images of the three crystals under UV irradiation.

3. Results and discussion

3.1 Crystal structures and emission properties of TMOE and TDMOE

Two types of single crystals of TMOE with different emission colours (TMOE-1: 420 nm; TMOE-2: 440 nm) were obtained (Fig. 1). Analysis of the intermolecular interactions in these crystals proves that no π - π interaction or any type of H or J-aggregation exist in either crystals due to the centrosymmetric and propeller shape (crystal structure of TMOE-1 and TMOE-2, see ESI†). Because the dihedral angles between the ethylene core and the four peripheral benzene groups in both crystals were not the same, and it is not easy to compare the difference in coplanarity as well as conjugation extend directly (Fig. S7, ESI†). Therefore, bond length alternation (BLA), a critical parameter determining the bandgap and conjugation of π -delocalized systems, is used for estimation of the conjugation difference in TMOE-1 and TMOE-2 based on the exact molecular conformations in the crystals.¹² BLA is calculated to be 0.03843 for TMOE-1, and 0.03830 for TMOE-2. The smaller BLA value for TMOE-2 suggests the better molecular coplanarity and conjugation.^{12,13} Furthermore, theoretical calculation on the bandgaps of TMOE-1 and TMOE-2 were performed using the B3LYP/6-31+g(d, p) basis set.¹⁴ It indicated the HOMO-LUMO bandgaps are 4.22 eV for TMOE-1 and 4.17 eV for TMOE-2 (Fig. S8, ESI†). Both the BLA and theoretical calculation results support that better conjugation in TMOE-2 is the main reason for the redshift of the emission compared with TMOE-1. As for TDMOE crystal (crystal structure of TDMOE, see ESI†), its emission peak is at 460 nm (Fig. 1). There is no π - π interaction or any type of H or J-aggregation is observed either, indicating the emission of the crystal is also a single molecular behavior. More evidences can be found in the following study on their optical properties in solution.

3.2 Optical properties of TMOE and TDMOE in THF, and THF/water binary solution: AIE and AIEE performances

THF is a good solvent for both TMOE and TDMOE, and water is a poor solvent. Adding water to the THF solution of these two molecules will cause the well-dissolved molecules to aggregate and result in an enhancement of emission. And this typical process is called AIE or AIEE properties.¹⁵ As seen in Fig. 2A, when water fraction (f_w) is lower than 80%, the

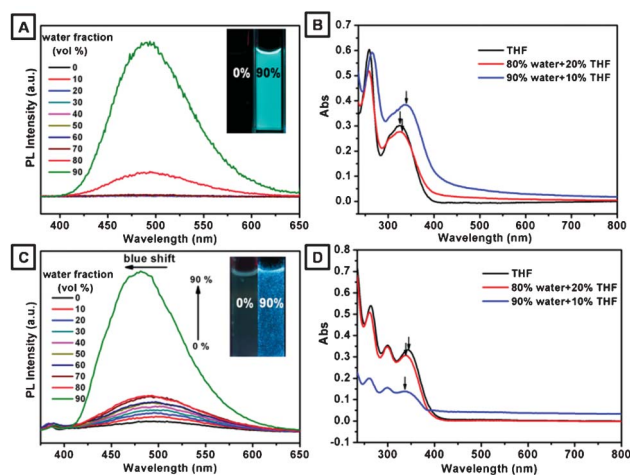


Fig. 2 (A) PL (Ex: 328 nm) and (B) UV-vis absorption spectra of TMOE (2×10^{-5} M) in THF/water mixtures with different water fractions (f_w). Inset: fluorescent photographs of TMOE in THF and THF/water mixtures ($f_w = 90\%$). (C) PL (Ex: 343 nm) and (D) UV-vis absorption spectra of TDMOE (2×10^{-5} M) in THF/water mixtures with different water fractions (f_w). Inset: fluorescent photographs of TDMOE in THF and THF/water mixtures ($f_w = 90\%$).

solution of TMOE has virtually no emission because of the free rotation of carbon-carbon single bonds between the four periphery phenyls and the ethylene core. Higher f_w than 80% leads to the aggregation of TMOE and the enhancement of its emission. The fact that aggregation has happened is deduced from the lifted spectral tails in UV-vis absorption spectra, which are caused by the Mie or light-scattering effect from nano-sized particles (Fig. 2B).¹⁶ Although it is hard to tell the change of TMOE conjugation state between in THF solution and water-induced aggregations from PL spectra, because TMOE hardly has emission in THF solution, UV-vis absorption spectra give right the information. The first absorption peak of TMOE red-shifts about 14 nm from 324 nm to 338 nm when the f_w increases from 0% to 90%, indicating a better conjugation in the water-induced aggregation.

Introduction of another four methoxy groups on the *ortho* position of methoxy of TMOE increases steric effect, resulting in the restriction of the rotation by the four periphery phenyls. Thus TDMOE have a weak emission at 494 nm in THF solution (Fig. 2C). The intensity of emission increases with the f_w . Meanwhile, the emission peak of the aggregated TDMOE blue-shifts 13 nm from 494 nm to 481 nm when the f_w increases from 0% to 90%. In the same way, the first absorption peak blue-shifts 6 nm from 343 nm to 337 nm as shown in Fig. 2D. So, the blueshift of both emission peak and absorption peak suggests that TDMOE in THF solution have better conjugation than in the water-induced aggregates. So far, it can be seen that TMOE and TDMOE have different conformational response upon poor solvent. Meanwhile, it can be clear seen that the conjugation state in water-induced aggregations of both TMOE and TDMOE is better than their crystals by comparing their emission peaks. The phenomena are very interesting, but the reason remains unclear, because the factors that affect the conformations are complex and it is difficult to make an easy conclusion.

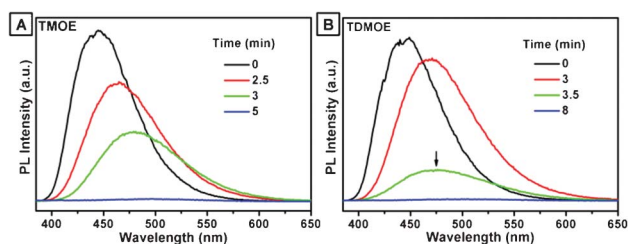


Fig. 3 Variation of PL spectra with time of TMOE (A) and TDMOE (B) in frozen THF solution (2×10^{-5} M) during their melting.

3.3 Emission properties in solidified solution

Another method to restrict the free rotation of a molecule and enable the fluorescence is freezing it at low temperature. This method was used to further investigate the single molecular conjugation state of TMOE and TDMOE in solutions. Frozen TMOE and TDMOE were obtained by solidifying their dilute THF solutions (2×10^{-5} M) with liquid nitrogen, and they show emission peaks at 448 nm and 442 nm, respectively. As the melting of the frozen THF, the emission peaks red-shift with the decreasing intensity (Fig. 3). This is consistent with literature reports that freezing of the fluorophore usually causes a blueshift in emission,¹⁷ because molecular rotation and vibration are forbidden, and the emission peak red-shifts with decreasing intensity as the melting of the solid. The emission peaks of TPE, TMOE-1, TMOE-2, and TDMOE in various conditions are summarized in Table 1.

Although the emission of frozen single molecular TMOE was measured at ~ 80 K, its emission peak is still longer than the crystals of TMOE-1 and TMOE-2. As the emission peak red-shifts with the melting of THF, it is safe to deduce that the TMOE solution has longer emission than its crystals, if it could be measured by steady-state fluorescence spectroscopy. As for TDMOE, when temperature increases to the melting temperature of THF, an emission peak at 475 nm is found (indicated by the arrow in Fig. 3B), which already red-shifts compared with the emission of its crystals. However, it is still hard to draw the conclusion that TMOE and TDMOE have better conjugation in solution than in crystals because of the existence of complex solvent effects.

Table 1 Summary of emission peaks of TPE, TMOE-1, TMOE-2, and TDMOE in various conditions

	TPE	TMOE-1	TMOE-2	TDMOE
Solution ^a (RT)	—	—	—	494
Aggregate ^b (RT)	463	—	492	488
Solidified solution ^c (83 K)	449	—	448	442
Crystal (RT)	447	420	440	460

^a THF solution (2×10^{-5} M). ^b Aggregates generated in THF/water mixtures ($f_w = 90\%$). ^c THF solution (2×10^{-5} M) frozen by liquid nitrogen.

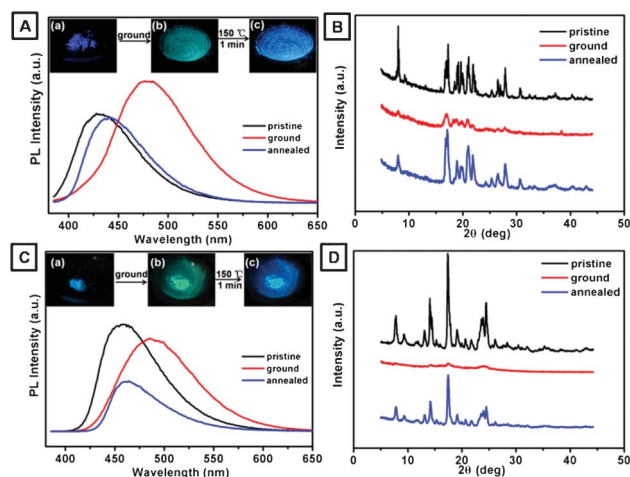


Fig. 4 PL spectra (A) and XRD patterns (B) of TMOE-1: pristine, ground and annealed sample (150 °C for 1 min). PL spectra (C) and XRD patterns (D) of TDMOE: pristine, ground and annealed sample (150 °C for 1 min). Insets: real object illustration of the process.

3.4 Emission shift from crystalline to amorphous state upon grinding: mechanofluorochromic performances

The strong fluorescence of TMOE-1 pristine crystals can change from blue (Em: 420 nm) to cyan (Em: 480 nm) by grinding. While, the emission peak of TMOE-2 crystal change from 440 nm to 487 nm after grinding. Similarly, the emission of TDMOE pristine crystal at 460 nm red-shifts to 480 nm after grinding. The fluorescence can almost go back to the original again upon thermal treatment (Fig. 4, Fig. S9, ESI†). XRD measurements show that the mechanofluorochromic properties are directly caused by crystalline to amorphous phase transition. Upon grinding, the crystalline structure convert to amorphous phase as indicated from the disappearance of XRD patterns. The reversible mechanofluorochromic behaviors can be repeated for many cycles. Deserving to be mentioned, the emission peaks of ground samples of TMOE-1 and TMOE-2 were not exactly the same, furthermore, the amorphous samples of TMOE-1 and TMOE-2 converted to TMOE-1 crystals and TMOE-2 crystals respectively upon heat-annealing, which indicating that the mechanofluorochromic performance of TMOE is related to the original crystal structure.

The change in aggregation state of TMOE-1 and TDMOE was further confirmed by DSC analysis (Fig. 5). There are two adjacent endothermic peaks at 176 °C and 187 °C for TMOE-1 pristine crystals. The former refers to the crystal phase conversion¹⁰ from TOME-1 to TMOE-2 (Fig. S10, ESI†), and the latter corresponds to melting point. After grinding, an exothermic peak at 55 °C appeared, indicating that the ground sample is in a metastable amorphous state and can recrystallize in the solid state by heating. The phenomenon is consistent with literature reports.¹⁸ However, the former endothermic peak became broader and shifts to 159 °C, suggesting the regenerated crystal structure induced by heat annealing is not as good as the original TMOE-1 crystallized in solution. After the amorphous TOME-1 was annealed at 150 °C for 1 min, the exothermic peak for the amorphous to TMOE-1

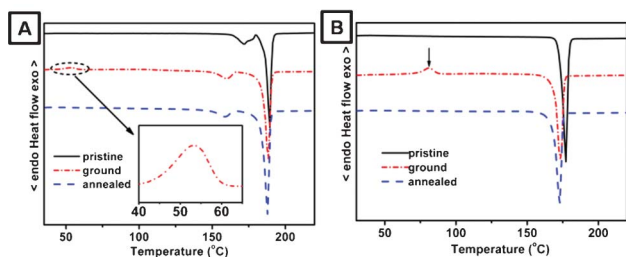


Fig. 5 DSC curves of TMOE-1 (A) and TDMOE (B): pristine, ground and annealed sample (150 °C for 1 min).

crystalline phase transition disappeared at 55 °C, and the endothermic peaks responsible for TMOE-1 to TMOE-2 phase transition and melting points resembled with the ground sample, indicating heat annealing at 150 °C for 1 min is still insufficient to generate good TMOE-1 crystals, that's why the fluorescence can not go back to the original 420 nm. If higher temperature was applied, it can be conjectured that crystal structure of TMOE-2 could be generated. As for TDMOE crystals, there is only one endothermic peak in DSC curve assigned to the melting point. The ground sample of TDMOE crystallized at 81 °C with correspondence to the exothermic peak as indicated by the arrow in Fig. 5B. Similarly, after heat annealing of the ground TDMOE at 150 °C for 1 min, the exothermic peak responsible for the amorphous to crystal transition disappears with a slightly lower melting points (Fig. 5B). The above results proved the crystalline to amorphous phase transition is the direct cause of the mechanofluorochromic behavior. And the more planar conformation and resultant better conjugation of single molecules in the amorphous state is the inherent reason for the fluorescence shift. Wetting with organic solvents is another way to transform the ground samples to crystals (Fig. S11, ESI†). However, heat annealing is more practical when applying these molecules on daily anti-counterfeiting applications.

Fluorescence decay experiments show that the lifetimes of all the crystals and their amorphous counterparts are all at a level of several nanoseconds. The very small changes in lifetime before and after grinding indicate that the molecular environments do not have significant change, and this also excludes the possibility of intermolecular π - π stacking after grinding (Fig. 6). Therefore, samples in crystalline and

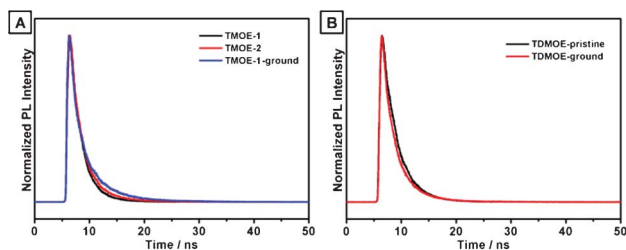


Fig. 6 Time-resolved emission decay curves of (A) TMOE-1, TMOE-2 and ground TMOE-1; (B) TDMOE crystal and ground TDMOE.

amorphous states shouldn't have significant change in quantum yields. Assuredly, integration sphere measurements prove these samples all have comparable high quantum yields, TMOE-1: 54%, TMOE-2: 60%, ground TMOE: 67%; TDMOE: 74%; ground TDMOE: 78%. Therefore, they all have potential applications in solid state stimuli-responsive materials with good optical response.

It is known that TPE does not have mechanofluorochromic properties, because it can not undergo a crystalline to amorphous phase transition (Fig. S12, ESI†). Although only small methoxy groups are substituted on TPE, more flexible intermolecular interactions of C-H \cdots O and C-H \cdots π are introduced (Fig. S13, ESI†). The flexible interactions make the sliding and deformation of the crystal structure easier, facilitating the transition from crystalline to amorphous phase. In contrast, TPE crystals with only rigid C-H \cdots π interactions between benzyl groups exhibit fragile character under external pressure or stimuli. Therefore, increment of relative "soft interaction" between the molecules is thought to be the essential factor for TPE derivatives which possess the mechanofluorochromic performance.¹⁰ Moreover, the weak interactions were thought to stabilize the metastable state of more planar conformation under pressure.

3.5 Application in anti-counterfeiting label in paper money

Fluorescent dyes have been incorporated onto paper money and used as anti-counterfeiting labels widely. Apparently, reversible mechanofluorochromic materials can further increase the security. TMOE, which has more obvious fluorescence change than TDMOE, was selected as anti-counterfeiting ink. Chinese "5 yuan" was printed onto a practice banknote to demonstrate the application (Fig. 7). The fluorescence of the characters have cyan fluorescence as soon as the THF solution of TMOE was sprayed on the paper because of the fast volatilization of solvent, and the molecular packing was in the *meta*-stable amorphous state in this situation. The molecules went to a more stable crystalline state after annealing treatment by IR light or heating on a hot plate, and the fluorescence change to blue. Selective grinding

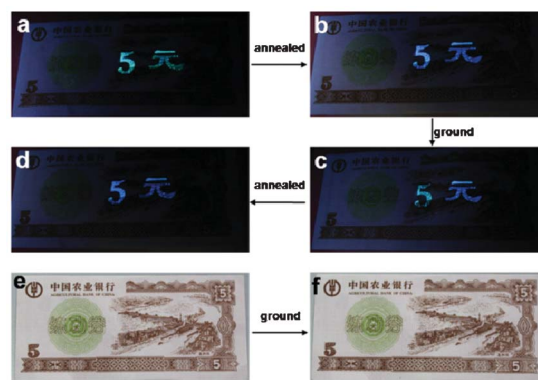


Fig. 7 Illustration of TMOE as an anti-counterfeiting ink on a 5-yuan RMB practice note printed with Chinese characters of "5-yuan". Images are (a) the note immediately after "5-yuan" was printed, (b) after annealed; (c) when 5 was ground (d) after annealed again under UV light irradiation. (e) and (f) are images of (b) and (c) under visible light, respectively.

the character “5” can cause an obvious color contrast with the unground “yuan”. There is no obvious change in the visible light before and after grinding as well as annealing because they don't have absorption in visible light range. Repeated annealing and grinding can be used to induce the responsive fluorescent color change and increase the complexity of the anti-counterfeiting performance compared with common fluorescent dyes. The reversible mechanofluorochromic process can be reproduced for many times. The results indicate this kind of material has practical applications in high security anti-counterfeiting inks.

4. Conclusions

Two methoxy-substituted TPE derivatives, TMOE and TDMOE, have been synthesized. Crystal structures and theoretical calculations both prove that their emissions are determined by single molecular conformation (or conjugation state) without intermolecular effects, such as H or J-aggregation and π - π stacking. Pure conformational effect on the molecular emissions has been studied in five environments of crystal(s), THF solution, THF-water binary solution, solidified THF and amorphous states. The response to these chemical environments enables TMOE and TDMOE to show AIE (AIEE) and mechanofluorochromic properties. In the absence of intermolecular effects, TMOE and TDMOE have comparable high quantum yields in crystalline and amorphous states. TMOE, which has better color contrast, has been used for anti-counterfeiting on banknotes, showing the practical applications of these materials in security inks.

Acknowledgements

We would like to thank Dr Minjie Li for fruitful discussions and generous support. We are grateful to the National Science Foundation of China (21072025) for financial support.

Notes and references

- (a) Q. Chen, D. Q. Zhang, G. X. Zhang, X. Y. Yang, Y. Feng, Q. H. Fan and D. B. Zhu, *Adv. Funct. Mater.*, 2010, **20**, 3244; (b) C. S. Zhu, S. P. Pang, J. P. Xu, L. Jia, F. M. Xu, J. Mei, A. J. Qin, J. Z. Sun, J. Ji and B. Z. Tang, *Analyst*, 2011, **136**, 3343; (c) Y. Q. Dong, J. W. Y. Lam, A. J. Qin, J. Z. Liu, Z. Li, B. Z. Tang, J. X. Sun and H. S. Kwok, *Appl. Phys. Lett.*, 2007, **91**, 011111; (d) H. Tong, Y. N. Hong, Y. Q. Dong, M. Häußler, J. W. Y. Lam, Z. Li, Z. F. Guo, Z. H. Guo and B. Z. Tang, *Chem. Commun.*, 2006, 3705.
- (a) J. D. Luo, Z. L. Xie, J. W. Y. Lam, L. Cheng, H. Y. Chen, C. F. Qiu, H. S. Kwok, X. W. Zhan, Y. Q. Liu, D. B. Zhu and B. Z. Tang, *Chem. Commun.*, 2001, 1740; (b) J. W. Chen, C. C. W. Law, J. W. Y. Lam, Y. P. Dong, S. M. F. Lo, I. D. Williams, D. B. Zhu and B. Z. Tang, *Chem. Mater.*, 2003, **15**, 1535; (c) Z. Li, Y. Q. Dong, B. X. Mi, Y. H. Tang, M. Häußler, H. Tong, Y. P. Dong, J. W. Y. Lam, Y. Ren, H. H. Y. Sung, K. S. Wong, P. Gao, I. D. Williams, H. S. Kwok and B. Z. Tang, *J. Phys. Chem. B*, 2005, **109**, 10061.
- (a) J. Huang, X. Yang, X. Li, P. Chen, R. Tang, F. Li, P. Lu, Y. Ma, L. Wang, J. Qin, Q. Li and Z. Li, *Chem. Commun.*, 2012, **48**, 9586; (b) J. Huang, X. Yang, J. Wang, C. Zhong, L. Wang, J. Qin and Z. Li, *J. Mater. Chem.*, 2012, **22**, 2478; (c) X. Xu, J. Huang, J. Li, J. Yan, J. Qin and Z. Li, *Chem. Commun.*, 2011, **47**, 12385; (d) Y. N. Hong, J. W. Y. Lam and B. Z. Tang, *Chem. Commun.*, 2009, 4332; (e) M. Wang, G. X. Zhang, D. Q. Zhang, D. B. Zhu and B. Z. Tang, *J. Mater. Chem.*, 2010, **20**, 1858; (f) Z. J. Zhao, S. M. Chen, X. Y. Shen, F. Mahtab, Y. Yu, P. Lu, J. W. Y. Lam, H. S. Kwok and B. Z. Tang, *Chem. Commun.*, 2010, **46**, 686; (g) Y. Hong, L. Meng, S. Chen, C. W. T. Leung, L. T. Da, M. Faisal, D. A. Silva, J. Liu, J. W. Y. Lam, X. Huang and B. Z. Tang, *J. Am. Chem. Soc.*, 2012, **134**, 1680; (h) Y. Hong, L. Meng, S. Chen, C. W. T. Leung, L. T. Da, M. Faisal, D. A. Silva, J. Liu, J. W. Y. Lam, X. Huang and B. Z. Tang, *J. Phys. Chem. B*, 2007, **111**, 11817; (i) Y. Liu, C. Deng, L. Tang, A. Qin, R. Hu, J. Z. Sun and B. Z. Tang, *J. Am. Chem. Soc.*, 2011, **133**, 660.
- (a) N. Zhao, Z. Y. Yang, J. W. Y. Lam, H. H. Y. Sung, N. Xie, S. J. Chen, H. M. Su, M. Gao, I. D. Williams, K. S. Wong and B. Z. Tang, *Chem. Commun.*, 2012, **48**, 8637; (b) J. Wang, J. Mei, R. Hu, J. Z. Sun, A. Qin and B. Z. Tang, *J. Am. Chem. Soc.*, 2012, **134**, 9956.
- (a) X. Zhang, Z. Chi, H. Li, B. Xu, X. Li, W. Zhou, S. Liu, Y. Zhang and J. Xu, *Chem.-Asian J.*, 2011, **6**, 808; (b) B. Xu, Z. Chi, J. Zhang, X. Zhang, H. Li, X. Li, S. Liu, Y. Zhang and J. Xu, *Chem.-Asian J.*, 2011, **6**, 1470; (c) H. Li, X. Zhang, Z. Chi, B. Xu, W. Zhou, S. Liu, Y. Zhang and J. Xu, *Org. Lett.*, 2011, **13**, 556; (d) H. Li, Z. Chi, B. Xu, X. Zhang, X. Li, S. Liu, Y. Zhang and J. Xu, *J. Mater. Chem.*, 2011, **21**, 3760; (e) B. Xu, Z. Chi, X. Zhang, H. Li, C. Chen, S. Liu, Y. Zhang and J. Xu, *Chem. Commun.*, 2011, **47**, 11080; (f) X. Zhang, Z. Chi, B. Xu, C. Chen, X. Zhou, Y. Zhang, S. Liu and J. Xu, *J. Mater. Chem.*, 2012, **22**, 18505; (g) B. Xu, M. Xie, J. He, B. Xu, Z. Chi, W. Tian, L. Jiang, F. Zhao, S. Liu, Y. Zhang, Z. Xu and J. Xu, *Chem. Commun.*, 2013, **49**, 273; (h) X. Zhou, H. Li, Z. Chi, X. Zhang, J. Zhang, B. Xu, Y. Zhang, S. Liu and J. Xu, *New J. Chem.*, 2012, **36**, 685.
- Z. Chi, X. Zhang, B. Xu, X. Zhou, C. Ma, Y. Zhang, S. Liu and J. Xu, *Chem. Soc. Rev.*, 2012, **41**, 3878.
- (a) M. Maus and W. Rettig, *Chem. Phys.*, 1997, **218**, 151; (b) Y. N. Hong, J. W. Y. Lam and B. Z. Tang, *Chem. Commun.*, 2009, 4332; (c) F. Chen, J. Zhang and X. Wan, *Chem.-Eur. J.*, 2012, **18**, 4558.
- (a) Z. Zhang, D. Yao, T. Zhou, H. Zhang and Y. Wang, *Chem. Commun.*, 2011, **47**, 7782; (b) N. Mizoshita, T. Tani and S. Inagaki, *Adv. Mater.*, 2012, **24**, 3350.
- (a) S. J. Yoon, J. W. Chung, J. Gierschner, K. S. Kim, M. G. Choi, D. Kim and S. Y. Park, *J. Am. Chem. Soc.*, 2010, **132**, 13675; (b) Y. Dong, B. Xu, J. Zhang, X. Tian, L. Wang, J. Chen, H. Lv, S. Wen, B. Li, L. Ye, B. Zou and W. Tian, *Angew. Chem., Int. Ed.*, 2012, **51**, 10782.
- X. Luo, W. Zhao, J. Shi, C. Li, Z. Liu, Z. Bo, Y. Q. Dong and B. Z. Tang, *J. Phys. Chem. C*, 2012, **116**, 21967.
- (a) X. F. Duan, J. Zeng, J. W. Lü and Z. B. Zhang, *J. Org. Chem.*, 2006, **71**, 9873; (b) T. S. Navale, L. Zhai, S. V. Lindeman and R. Rathore, *Chem. Commun.*, 2009, 2857.

- 12 S. Ohira, J. M. Hales, K. J. Thorley, H. L. Anderson, J. W. Perry and J. L. Brédas, *J. Am. Chem. Soc.*, 2009, **131**, 6099.
- 13 S. Yang and M. Kertesz, *J. Phys. Chem. A*, 2006, **110**, 9771.
- 14 M. J. Frisch, G. W. Trucks, H. B. Schlegel, G. E. Scuseria, M. A. Robb, J. R. Cheeseman, G. Scalmani, V. Barone, B. Mennucci, G. A. Petersson, H. Nakatsuji, M. Caricato, X. Li, H. P. Hratchian, A. F. Izmaylov, J. Bloino, G. Zheng, J. L. Sonnenberg, M. Hada, M. Ehara, K. Toyota, R. Fukuda, J. Hasegawa, M. Ishida, T. Nakajima, Y. Honda, O. Kitao, H. Nakai, T. Vreven, J. Montgomery Jr., J. E. Peralta, F. Ogliaro, M. Bearpark, J. J. Heyd, E. Brothers, K. N. Kudin, V. N. Staroverov, R. Kobayashi, J. Normand, K. Raghavachari, A. Rendell, J. C. Burant, S. S. Iyengar, J. Tomasi, M. Cossi, N. Rega, J. M. Millam, M. Klene, J. E. Knox, J. B. Cross, V. Bakken, C. Adamo, J. Jaramillo, R. Gomperts, R. E. Stratmann, O. Yazyev, A. J. Austin, R. Cammi, C. Pomelli, J. W. Ochterski, R. L. Martin, K. Morokuma, V. G. Zakrzewski, G. A. Voth, P. Salvador, J. J. Dannenberg, S. Dapprich, A. D. Daniels, O. Farkas, J. B. Foresman, J. V. Ortiz, J. Cioslowski and D. J. Fox, Gaussian 09, (Revision A. 02), Gaussian, Inc., Wallingford, CT 2009.
- 15 W. Z. Yuan, F. Mahtab, Y. Gong, Z. Q. Yu, P. Lu, Y. Tang, J. W. Y. Lam, C. Zhu and B. Z. Tang, *J. Mater. Chem.*, 2012, **22**, 10472.
- 16 B. Z. Tang, Y. Geng, J. W. Y. Lam, B. Li, X. Jing, X. Wang, F. Wang, A. Pakhomov and X. X. Zhang, *Chem. Mater.*, 1999, **11**, 1581.
- 17 (a) M. A. El-Bayoumi and F. M. A. Halim, *J. Chem. Phys.*, 1968, **48**, 2536; (b) F. D. Lewis and W. Liu, *J. Phys. Chem. A*, 2002, **106**, 1976.
- 18 X. Luo, J. Li, C. Li, L. Heng, Y. Q. Dong, Z. Liu, Z. Bo and B. Z. Tang, *Adv. Mater.*, 2011, **23**, 3261.